NeuroImage 327 (2026) 121759

Contents lists available at ScienceDirect

NeuroImage

journal homepage: www.elsevier.com/locate/ynimg

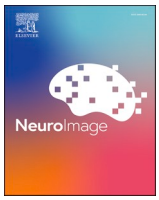

Evidence for enhanced backward connectivity in the third visual pathway following cortico-cortical paired associative stimulation

Gabriele Pirazzini [a,*], Antonio Cataneo [b], Silvana Pelle [a], Alice Marra [b], Giorgio Arcara [c,d], Simone Battaglia [e,f], Mauro Ursino [a,#], Alessio Avenanti [b,g,#]

[a] Department of Electrical, Electronic and Information Engineering "Guglielmo Marconi", University of Bologna, Cesena, Italy
[b] Center for Studies and Research in Cognitive Neuroscience, Department of Psychology "Renzo Canestrari", University of Bologna, Cesena, Italy
[c] Department of General Psychology, University of Padua, Padova, Italy
[d] San Camillo IRCCS Hospital, Venezia, Italy
[e] Department of Theoretical and Applied Sciences, eCampus University, Novedrate (Como), Italy
[f] Department of Psychology, University of Turin, Torino, Italy
[g] Center for Research in Neuropsychology and Cognitive Neuroscience (CINPSI Neurocog), Universidad Católica Del Maule, Talca, Chile

ARTICLE INFO

Keywords:
Third visual pathway
ccPAS
EEG
Granger causality
Functional connectivity
Associative plasticity

ABSTRACT

The posterior superior temporal sulcus (pSTS) and early visual cortex (V1/V2) form part of a lateral occipito-temporal network - proposed as a "third" visual pathway - supporting the processing of socially and emotionally relevant information. Prior studies using cortico-cortical paired associative stimulation (ccPAS) applied from pSTS to V1/V2 have shown enhanced recognition of facial emotional expressions, interpreted as reflecting strengthened temporo-occipital backward connectivity. However, direct evidence that ccPAS can modulate pSTS-to-V1/V2 connectivity has been lacking. Here, we applied ccPAS consisting of repeated paired TMS pulses, with the first pulse delivered over pSTS and the second pulse over V1/V2 ($ccPAS_{STS\text{-}V1}$). A reverse-order protocol ($ccPAS_{V1\text{-}STS}$) served as a control. Resting-state EEG was recorded before, immediately after, and 30 min post-stimulation to assess functional connectivity. Multivariate spectral Granger Causality analysis characterized the directionality and frequency-dependent dynamics of connectivity. Outdegree metrics revealed that $ccPAS_{STS\text{-}V1}$ enhanced backward functional connectivity immediately after stimulation, with effects persisting after 30 min, possibly consistent with Hebbian-like associative plasticity in top-down pathways. In addition, an increase in forward connectivity was observed 30 min after $ccPAS_{V1\text{-}STS}$, and more weakly after $ccPAS_{STS\text{-}V1}$, possibly reflecting broader compensatory mechanisms. These findings demonstrate that ccPAS can transiently and selectively modulate directional connectivity within the "third" visual pathway, providing insights into the physiological basis of ccPAS and suggesting that previously observed improvements in emotion recognition following $ccPAS_{STS\text{-}V1}$ may arise from plastic changes in backward pSTS-to-V1/V2 connectivity. More broadly, they underscore the potential of ccPAS to probe and modulate the dynamics of higher-order visual circuits.

1. Introduction

Human vision is not a simple feedforward cascade. After a first sweep of sensory information, higher-order cortices rapidly send feedback signals that refine and contextualize activity in early visual areas (Lamme and Roelfsema, 2000; Summerfield and de Lange, 2014; Michel et al., 2019). An example is the loop linking the right posterior superior temporal sulcus (pSTS) - considered to be the endpoint of a "third" occipito-temporal pathway (Pitcher and Ungerleider, 2021; Weiner and Gomez, 2021) that complements the ventral and dorsal streams (Milner and Goodale, 2006), and is dedicated to social and emotional perception - with the primary/secondary visual cortex (V1/V2), where the earliest cortical representation of visual features emerges. Converging structural and functional data show that pSTS and V1/V2 are mutually interconnected through both direct projections and polysynaptic pathways (D. Boussaoud et al., 1990; Distler et al., 1993; K. S. Rockland and Van Hoesen, 1994; Pitcher et al., 2011; Weiner et al., 2016). Analysis of functional connectivity shows that the strength of functional coupling

* Corresponding author.
E-mail address: gabriele.pirazzini3@unibo.it (G. Pirazzini).
# These authors contributed equally as last authors.

https://doi.org/10.1016/j.neuroimage.2026.121759
Received 3 November 2025; Received in revised form 26 January 2026; Accepted 26 January 2026
Available online 27 January 2026

between the pSTS and V1/V2 predicts individual differences in the recognition accuracy of emotional expressions (Wang et al., 2016). Remarkably, evidence suggests that backward pathways from pSTS to V1/V2 play a critical role in emotion perception. Using transcranial magnetic stimulation (TMS), we demonstrated that enhancing pSTS–V1/V2 connectivity through cortico-cortical paired associative stimulation (ccPAS) improves performance in tasks requiring the discrimination of emotional expressions from faces (Borgomaneri et al., 2023; Cataneo et al., submitted). The ccPAS protocol consists of the repeated administration of paired TMS pulses to two target regions, with an interstimulus interval (ISI) chosen to match the estimated elaboration delay between them (Di Luzio et al., 2024). This temporal alignment mimics neural firing known to induce Hebbian-like spike-timing-dependent plasticity (STDP), thereby strengthening synaptic efficacy across the stimulated pathway (Hernandez-Pavon et al., 2023a; Rizzo et al., 2009; Turrini and Avenanti, 2023).

To design a ccPAS protocol to target backward connections from pSTS to V1/V2, in our previous study, we combined TMS and electroencephalography (EEG) to estimate the timing of interactions from pSTS to V1/V2 (Borgomaneri et al., 2023). When we stimulated the pSTS, we found that V1/V2 responded maximally about 200 ms later, revealing long-latency pSTS-to-V1/V2 interactions at rest. Building on this, we designed a long-latency ccPAS protocol designed to repeatedly activate pSTS (first pulse) and V1/V2 (second pulse) with an ISI matching these long-range pSTS-V1/V2 communication delays (200 ms). This $ccPAS_{STS\text{-}V1}$ protocol modulated the amplitude of the P1 and N170 components elicited by emotional faces, with the strongest effects over the targeted temporo-occipital areas (Borgomaneri et al., 2023; Cataneo et al., submitted); moreover, $ccPAS_{STS\text{-}V1}$ improved recognition of emotional expressions (Borgomaneri et al., 2023). These findings suggest that backward connections from pSTS to V1/V2 are malleable, can undergo Hebbian-like potentiation, and play a crucial role in emotion perception (Borgomaneri et al., 2023; Cataneoet al., submitted). In contrast, no behavioral or electrophysiological changes were observed when the protocol was applied in the reverse direction ($ccPAS_{V1\text{-}STS}$), or with mismatched ISIs (Borgomaneri et al., 2023). While these findings provide compelling evidence that ccPAS can modulate the pSTS-V1/V2 pathway in a functionally meaningful way, the underlying neural mechanisms remain poorly understood. In particular, these studies do not directly elucidate how ccPAS alters the dynamics of information transmission between pSTS and V1/V2, as no connectivity metrics were assessed.

Accumulating data demonstrate that ccPAS can impact connectivity strength in a direction-specific manner across multiple cortical pathways (Di Luzio et al., 2024). However, with few exceptions (e.g., (Chiappini et al., 2020)), prior studies have employed very short ISIs tailored to target fast, mainly direct cortico-cortical projections. No study to date has systematically investigated the impact of long-latency ccPAS, such as the protocol we developed to engage backward pSTS-to-V1/V2 projections. Although our long-latency $ccPAS_{STS\text{-}V1}$ protocol was designed to enhance communication along this pathway, direct evidence for direction-specific modulation of such connections is still missing.

Advanced neuroimaging techniques capable of capturing real-time neural interactions are essential to address these limitations. The high temporal resolution of EEG is well suited to track rapid fluctuations in neural activity, while computational methods such as cortical source reconstruction can mitigate its low spatial resolution by localizing the regions generating the observed signals. Furthermore, functional connectivity measures such as Granger Causality allow estimation of frequency-specific, weighted, and directional interactions between cortical regions, thereby providing insights into the dynamics of large-scale networks (Ginter et al., 2001; Bastos et al., 2015; Seth et al., 2015).

In the present work, we aimed to characterize how ccPAS shapes the intrinsic spatio-temporal dynamics of the pSTS-V1/V2 network. Healthy participants received a $ccPAS_{STS\text{-}V1}$ protocol previously shown to improve emotion recognition and modulate electrophysiological responses elicited by emotional faces, presumably by strengthening backward pSTS-to-V1/V2 projections (Borgomaneri et al., 2023; Cataneoet al., submitted). As a control condition, participants underwent the reverse protocol (i.e., $ccPAS_{V1\text{-}STS}$), which in prior work did not affect electrophysiological or behavioral response (Borgomaneri et al., 2023; Cataneoet al., submitted). To test the effect of ccPAS on cortico-cortical connectivity, in each session, resting-state EEG was recorded immediately before, immediately after, and 30 min post-ccPAS.

Source reconstruction was performed to identify cortical generators of the EEG signal, and functional connectivity across frequency bands was estimated using multivariate spectral Granger Causality. By assessing frequency-dependent directional influences among cortical regions, graph theory-based metrics provide a means to disentangle forward and backward components within large-scale cortical networks (Barnett and Seth, 2014). To summarize directional changes, we computed an *Outdegree index* (Rubinov and Sporns, 2010; Farahani et al., 2019), which quantifies the total strength of information a node transmits to other regions by summing the weights of its outgoing edges (Huang et al., 2016; van Mierlo et al., 2018). Here, this index was used to assess the extent to which temporoparietal regions surrounding pSTS exert backward influences on occipital areas (e.g., V1/V2), and vice versa. This approach provides a principled framework to capture the net directionality of information flow and to test whether ccPAS selectively enhances backward versus forward connectivity.

Based on our previous findings (Borgomaneri et al., 2023), and the principle of Hebbian-like plasticity thought to underlie ccPAS (Di Luzio et al., 2024), we hypothesized that $ccPAS_{STS\text{-}V1}$ would induce plastic changes, expressed as an increase in backward connectivity from pSTS to V1/V2. In contrast, reversing the stimulation order ($ccPAS_{V1\text{-}STS}$) was expected to exert little or no effect on backward connectivity and rather affect forward connectivity.

2. Methods

2.1. Participants

Twenty healthy young adult humans (11 females, mean age ± standard deviation: 24.3 ± 3.3 years) took part in the study. They were right-handed, had normal or corrected to normal vision, and were screened for contraindications to TMS (Rossi et al., 2009, 2021), including a history of neurological or psychiatric disorders and current use of psychotropic medication. No participant reported such conditions. Participants gave their written informed consent, but no formal questionnaires assessing subclinical depressive or anxiety symptoms were administered. The University of Bologna's Bioethics Committee approved the procedures, ensuring they adhered to the ethical standards outlined in the Declaration of Helsinki (World Medical Association, 2013). No discomfort or adverse effects from TMS were observed or reported throughout the experimental sessions.

2.2. Experimental design

Participants underwent two sessions of ccPAS protocol presented in a single-blinded and counterbalanced order on different days, with an interval of at least 7 days between sessions for washout (Hernandez-Pavon et al., 2023b): in one session, stimulation was delivered from pSTS to V1/V2 ("$ccPAS_{STS\text{-}V1}$" protocol), whereas in the other the order of the stimulation pulses was reversed ("$ccPAS_{V1\text{-}STS}$") (see "*ccPAS protocol*" below and (Borgomaneri et al., 2023) for more details). For each session, the primary outcome consisted of EEG recordings during three different 5-min eyes-open resting-state periods: just before the stimulation protocol ("*pre*" time interval), immediately after ("$post_{0min}$"), and 30 min post stimulation ("$post_{30min}$"). These measures were recorded to investigate potential changes in

cortico-cortical connectivity within the pSTS-V1/V2 network induced by the ccPAS protocols. A schematic illustration of the experimental design is depicted in Fig. 1. In addition to resting-state EEG, participants also completed an emotion recognition task (differentiating between facial expressions of fear and happiness) and underwent single-pulse TMS–EEG blocks at rest during each session. These behavioral and TMS-EEG data will not be presented in this manuscript, as they address questions that go beyond the specific focus on resting-state Granger connectivity in the present study.

2.3. ccPAS protocol

The ccPAS protocols were delivered with a monophasic Magstim BiStim2 machine (Magstim Company, UK) using two 50-mm figure-of-eight coils positioned over the right pSTS and V1/V2. For both stimulation sites, coils were positioned tangentially to the scalp. The coil over the pSTS site was oriented to induce an anteroposterior (AP) current in the underlying tissue directed toward the occipital target (V1/V2). Conversely, the coil over V1/V2 was oriented to induce an AP current directed toward the temporal target (pSTS). A total of 90 stimulus pairs were administered continuously at 0.1 Hz for ~15 min (Buch et al., 2011; Johnen et al., 2015; Romei et al., 2016; Fiori et al., 2018; Chiappini et al., 2018, 2020; Di Luzio et al., 2022; Turrini et al., 2022; Borgomaneri et al., 2023). In the ccPAS$_{STS\text{-}V1}$ protocol, the first pulse was delivered over pSTS, followed 200 ms later by a second pulse over V1/V2, whereas in the ccPAS$_{V1\text{-}STS}$ protocol, we used the same 200-ms ISI, but the order of the two pulses was reversed. The 200-ms ISI corresponds to the estimated temporal window for physiological signal processing from pSTS to V1/V2 (Borgomaneri et al., 2023). Thus, in the ccPAS$_{STS\text{-}V1}$ protocol, neurons in V1/V2 are first preactivated by the remote input elicited through pSTS stimulation and subsequently receive a direct exogenous input from the second TMS pulse over V1/V2. This temporal convergence of pre- and postsynaptic activation is thought to mimic the conditions that induce Hebbian-like spike-timing-dependent plasticity (STDP) (Caporale and Dan, 2008). By contrast, the same ISI is unlikely to optimally capture the dynamics of the reverse pathway, as no behavioral or neural effects have been reported in previous studies using ccPAS$_{V1\text{-}STS}$ (Borgomaneri et al., 2023; Cataneoet al., submitted). For this reason, this protocol serves as a suitable control condition. The intensity of the magnetic pulses was set at 60 % of the maximum stimulator output (MSO) (Borgomaneri et al., 2023; Di Luzio et al., 2024; Di Luzio et al., 2022; Tarasi et al., 2024). The pulses were triggered remotely using a computer that controlled both stimulators. We selected 60% MSO to match our prior work employing the same ccPAS protocol and stimulation sites, where this setting was shown to be safe and effective in producing robust physiological and behavioral effects (Borgomaneri et al., 2023), and because many ccPAS studies targeting associative plasticity in non-motor networks adopt fixed intensities for feasibility and consistency across ccPAS protocols (e.g. Di Luzio et al., 2024).

2.4. Neuronavigation

The placement of the two coils over pSTS and V1/V2 sites was defined individually for each participant using the SofTaxic Neuronavigation System (Electro Medical Systems). For neuronavigation, standard cranial landmarks (nasion, inion, and the two preauricular points) together with ~80 additional points uniformly distributed across the scalp were digitized with a Polaris Vicra system (Northern Digital). For each subject, an estimated individual MRI was generated by fitting a high-resolution MRI template to the participant's scalp model and cranial landmarks through a 3D warping procedure. The right pSTS site was localized at Talairach coordinates x=53, y=−49, z=10, derived from subject-weighted mean coordinates reported in a recent meta-analysis (Dricu and Frühholz, 2016). V1/V2 was identified by selecting the scalp location corresponding most closely to early visual cortex coordinates (x=19, y=−98, z=1). These anatomical targets were the same as those used in our previous ccPAS work (Borgomaneri et al., 2023; Cataneoet al., submitted) and are in line with earlier TMS studies focusing on pSTS (Avenanti et al., 2013; Candidi et al., 2015; Ferrari et al., 2018; Paracampo et al., 2018; Pitcher, 2014) and V1/V2 (Bertini et al., 2010; Avenanti et al., 2012; Breveglieri et al., 2021).

2.5. EEG preprocessing

Resting-state EEG signals were offline preprocessed via the EEGLAB v2022.0 MATLAB toolbox (Delorme and Makeig, 2004). Signals were collected at a sampling frequency of 1000 Hz and subsequently down-sampled to 250 Hz, bandpass filtered between 1 and 100 Hz, and notch filtered from 48 to 52 Hz (via linear zero-phase non-causal FIR filters). The tracings of each subject were then decomposed into 32 independent components via ICA (Bell and Sejnowski, 1995), in order to identify and remove artefactual components. Unique, non-stereotyped artifacts such as eye blinks were removed by visual inspection. Bad epochs (the ones presenting huge rubbing artifacts or undefined significant noise) were also removed. These pre-processing steps were

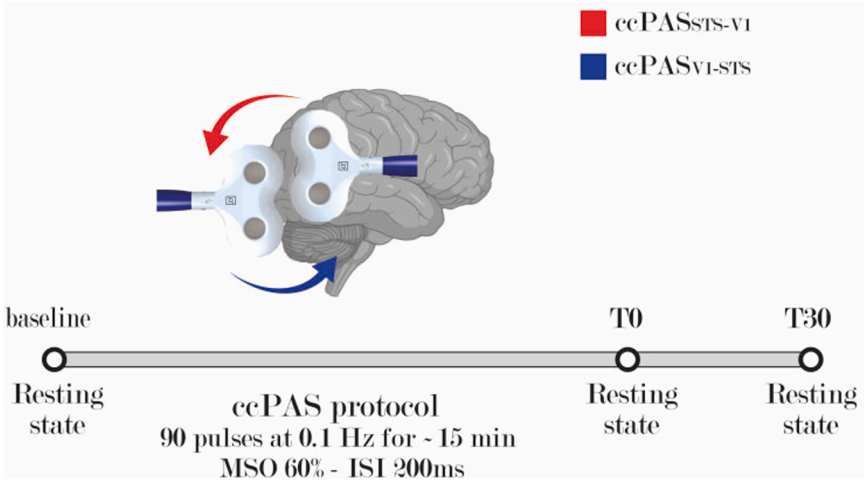

Fig. 1. *Schematic representation of the experimental design.* Surface EEG was recorded during three 5-min eyes-open resting-state blocks, immediately before ccPAS ("*pre*", baseline), immediately after ("*post$_{0min}$*", T0), and 30 min later ("*post$_{30min}$*", T30). Each participant completed two ccPAS sessions, one supposedly enhancing the pSTS-to-V1/V2 pathway (ccPAS$_{STS\text{-}V1}$) and a control condition (ccPAS$_{V1\text{-}STS}$).

performed blind to both the conditions and the time intervals.

2.6. Cortical source reconstruction

Cortical source activity was reconstructed starting from the pre-processed EEG signals. Intracortical current densities were computed employing the Brainstorm MATLAB toolbox (Tadel et al., 2011). A template three-layer head model (ICBM152 MNI template, which subdivides the cortex into 15,002 vertices) was used to address the forward problem. We solved the forward problem involving the Boundary Element Method within the OpenMEEG software (Gramfort et al., 2010). For estimating cortical sources, we adopted the standardized sLORETA algorithm, a linear inverse solution method for 3D EEG distributed source modeling (Pascual-Marqui, 2002). The algorithm computes a weighted minimum norm solution, in which the localization inference relies on standardized estimates of current density. The resulting solution is instantaneous, distributed, discrete, and linear and is presented with zero dipole localization error under ideal conditions (i.e., noise-free). We considered constrained dipole orientations, arranged perpendicularly to the cortical surface. For each participant, time interval, and session, we extracted the resting-state time series of standardized current densities for all 15,002 vertices. Subsequently, the cortical vertices were grouped based on the Brainnetome Atlas (Fan et al., 2016), which defines 246 regions of interest (*ROIs*) of the bilateral hemispheres. Within each *ROI*, the activities of the vertices were averaged at each time point, thereby resulting in a singular time series representative of the cortical *ROI* activity.

2.7. Multivariate spectral Granger Causality functional connectivity analysis

Starting from the Talairach coordinates of the two stimulation sites (for *pSTS:* x=53, y=−49, z=10; for *V1/V2:* x=19, y=−98, z=1) (see (Borgomaneri et al., 2023)), we identified 11 *ROIs* for the functional connectivity analysis based on the Brainnetome Atlas. Specifically, we selected the six parcels located closest to the *pSTS* stimulation site (*temporoparietal* cluster) and the five parcels located closest to the *V1/V2* stimulation site (*occipital* cluster). These *ROIs* are depicted in Fig. 2.

Functional connectivity analysis was performed across the 11 selected *ROIs*. Because resting-state GC relies on approximate signal stationarity, signals were first standardized with unit variance and zero mean to achieve data stationarity (Tawakuli et al., 2025). Then, we applied a multivariate spectral Granger Causality estimator (MVGC MATLAB toolbox (Barnett and Seth, 2014)), which yields weighted and directional metrics of causal interactions between *ROIs* across the entire signal's frequency spectrum. Multivariate spectral Granger Causality (GC) was subsequently employed to allow the mitigation of spurious causal inferences by accounting for joint dependencies from additional variables, thereby providing a more robust assessment of complex brain network interrelationships than a simple bivariate approach (Pelle et al., 2025). For each session, time interval, and participant, the multivariate spectral GC was computed for all *ROI* pairs and in both directions. Model-order selection was performed following Akaike and Bayesian Information Criteria analyses (Hlaváčková-Schindler and Plant, 2020). AIC and BIC values were computed for orders ranging from 1 to 100. The order p of the model was therefore set to 25, as an optimal compromise between model fit and parsimony. Accordingly, GC estimated values remain relatively stable for $p \geq 25$ (this value is also in line with our previous studies (Ursino et al., 2022; Pirazzini et al., 2023)). The computation provided an 11×11 connectivity matrix for each frequency sample (with auto-loops equal to zero). The spectral connectivity matrix for each participant was first averaged within the 4–80 Hz frequency range (from the lower bound of the theta band to the upper bound of the low-mid gamma band), obtaining an 11×11 connectivity matrix for each session ($ccPAS_{STS\text{-}V1}$ and $ccPAS_{V1\text{-}STS}$), time interval (*pre, post*$_{0min}$, and *post*$_{30min}$), and participant. Subsequently, the same procedure was repeated for each frequency band (4–8 Hz for theta, 8–12 Hz for alpha, 12–30 Hz for beta, and 30–80 Hz for low-mid gamma). Finally, outliers were identified and then removed using the interquartile range method, where single connectivity values falling outside $Q1 - 1.5 \times IQR$ and $Q3 + 1.5 \times IQR$ were excluded from further analyses.

The previous procedure provided one matrix per participant in each frequency band. To identify significant connections a two-tailed Monte Carlo non-parametric permutation *t*-test (5000 permutations) was employed for each session, comparing "*pre*" vs. "*post*$_{0min}$" and "*pre*" vs. "*post*$_{30min}$" matrices (Metropolis and Ulam, 1949). Significantly different connections were defined as those having a corrected *p*-value lower than 0.05 (False Discovery Rate correction, Benjamini-Hochberg procedure (Benjamini and Hochberg, 1995)). Consequently, among the possible 11×11 connections, solely the significantly different connections between *pre* and *post*$_{0min}$ (between *pre* and *post*$_{30min}$) time intervals were retained, while all non-significant connections were set to zero. This is a procedure commonly used in connectivity analysis (van den Heuvel et al., 2017; Pirazzini et al., 2023), and from this point onward, we referred to these matrices as "*sparse*". In conclusion, we obtained thirty sparse matrices with dimensions 11×11: one for each ccPAS protocol

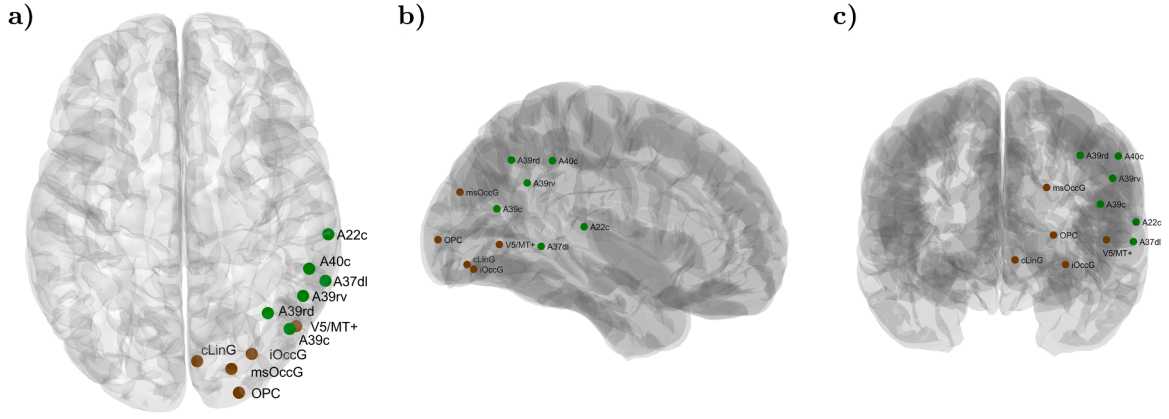

Fig. 2. *Selected cortical regions.* Selected ROIs from the Brainnetome Atlas for functional connectivity analysis: panel a) top view; panel b) lateral view; panel c) bottom view. A40c: caudal area 40 (MNI coordinates: 55.8; −43.81; 42.43); A22c: caudal area 22 (64.56; −27.73; 10.85); A39rv: rostroventral area 39 (52.88; −54.62; 30.44); A37dl: dorsolateral area 37 (62.6; −47.25; 0.79); A39rd: rostrodorsal area 39 (37.35; −62.22; 41.21); A39c: caudal area 39 (47.05; −69.32; 17.42); cLingG: caudal Lingual Gyrus (6.33; −82.18; −10.56); msOccG: medial superior Occipital Gyrus (20.84; −86.64; 24.15); iOccG: inferior Occipital Gyrus (30.57; −78.38; −12.44); OPC: Occipital Polar Cortex (24.72; −96.64; 0.29); V5/MT+: area V5/MT+ (49.97; −67.59; 0.59). ROIs of the temporoparietal cluster are depicted in green, while those of the occipital cluster in brown.

(ccPAS$_{STS\text{-}V1}$, ccPAS$_{V1\text{-}STS}$), time interval (*pre, post$_{0min}$*, and *post$_{30min}$* time intervals), and frequency band (entire frequency range, theta, alpha, beta, and gamma bands) by averaging the *sparse* connectivity matrices over the 20 participants. All analyses described in *Section 3.1* will be carried out on these *sparse* matrices.

Finally, the interconnections among all cortical *ROIs* have been depicted as a weighted graph, using the *difference* between the connectivity values at time *post$_{0min}$* and *pre* (or the difference between the connectivity values at *post$_{30min}$* and *pre*). The edge's weight denotes these connectivity differences, while the *ROIs* are the graph's nodes (Minati et al., 2013).

2.8. Analysis of backward and forward connectivity

To investigate the specificity of neurophysiological effects induced by the two ccPAS protocols, we focused primarily on long-range connectivity between the two clusters, thus excluding within-cluster connections. By *long-range connectivity* we mean connectivity between spatially distant cortical regions, specifically the *occipital* and the *temporoparietal* lobe. These areas are not only anatomically separate, but also hierarchically distinct within the visual system. In particular, we analyzed changes in backward connectivity (i.e., from temporoparietal to occipital ROIs) and forward connectivity (i.e., from occipital to temporoparietal ROIs) using a fundamental index taken from graph-theory: the *Outdegree* (Van Steen, 2010). *Outdegree* quantifies the influence of one cluster on another, defined as the sum of edge weights from all ROIs in one of the two clusters projecting to the second. In short, it reflects the extent to which a region sends information to another.

Outdegree values depend on the number of connections exiting a cluster. The greater the number of connections, the greater the outdegree. Hence, to make the comparisons uniform among different conditions, for each frequency band, we selected all connections present in at least one of the *sparse* matrices obtained in the previous analysis: i.e., a connection that survived at least one of the four previous permutation tests (*pre* vs *post$_{0min}$* and *pre* vs *post$_{30min}$*, for both ccPAS sessions). This procedure yielded less-sparse matrices, in which a connection is set to zero only if it was never significant in any of the four tests. Consequently, the total number of connections is constant in all tests; this ensures that the *Outdegree* interpretation is not influenced by different matrix sparsities, but rather by actual changes in connectivity strength, reinforcing confidence in our network-level conclusions. For each session, participant, time interval, and frequency band, we computed the *Outdegree* of the *temporoparietal* cluster and the *Outdegree* of the *occipital* cluster. Therefore, we evaluated the sum of the outgoing connections from all *ROIs* belonging to one cluster and entering the other. We will call this set of connections *backward* and *forward* connectivity.

To assess the significance of the results, in *Section 3.2* we statistically evaluated changes in inter-cluster *Outdegree* both within the same stimulation protocol (i.e., across different time intervals, *pre* vs *post$_{0min}$* and *pre* vs *post$_{30min}$*) and between the two different sessions (ccPAS$_{STS\text{-}V1}$ vs ccPAS$_{V1\text{-}STS}$, at both *post$_{0min}$* and *post$_{30min}$* time intervals). These comparisons were made for each considered frequency band. Note that when we compared the two ccPAS sessions, we did not compare the absolute values of *Outdegree* at *post$_{0min}$* and *post$_{30min}$*, but rather their differences from the relative values at *pre* (i.e., immediately before the stimulation protocol). This choice was made to assess which session showed the greatest change in connectivity, rather than which had the higher absolute values in inter-cluster connections.

Finally, although the main focus of this study was to investigate long-range connectivity between clusters, we also evaluated changes in intra-cluster connectivity between the two sessions for the entire frequency band. This was done to determine whether stimulation protocols exert a direct influence within clusters and whether this depends on the order of stimulation.

All statistical comparisons were performed via paired samples *t*-tests to evaluate *t*- and *p*-statistics. To further characterize the magnitude of the observed effects, effect-size estimates (Cohen's *d* and partial eta-squared η_p^2) were also computed. To account for the risk of Type I errors due to multiple testing, *p*-values were Bonferroni-corrected for 4 comparisons. Moreover, to test for possible order or carryover effects, a preliminary 2×2 mixed-design ANOVA was performed on the baseline (*"pre"*) *Outdegree* data. The analysis revealed neither a significant main effect of order nor a condition×order interaction.

3. Results

3.1. Graph analysis

Fig. 3 displays the functional connectivity analysis results for the entire 4–80 Hz frequency band. Results show a significant increase in functional connectivity from the temporal cluster after the ccPAS$_{STS\text{-}V1}$ protocol. This increase, which especially concerns the backward direction, is already noticeable immediately after the stimulation (*post$_{0min}$*), and becomes more pronounced after 30 min. Conversely, ccPAS$_{V1\text{-}STS}$ induced only minor connectivity changes at time *post$_{0min}$*. After 30 min, a network of mainly feedforward connections also begins to develop for the ccPAS$_{V1\text{-}STS}$ protocol.

3.2. Outdegree analysis

Results of the statistical comparisons between the *Outdegree* values in the temporoparietal and occipital clusters are reported in Fig. 4 for the entire frequency range. The comparisons across time intervals (Fig. 4, *panel a)* and *panel b)*) reveal a statistically significant increase in backward *Outdegree* only after ccPAS$_{STS\text{-}V1}$; this increase was already present at *post$_{0min}$* and still consistent at *post$_{30min}$*. Conversely, an increase in forward connectivity was found for both protocols, but only after 30 min. The comparison between the two sessions (Fig. 4 *panel c)*) shows that the increase in *Outdegree* for backward connections is significantly greater for the ccPAS$_{STS\text{-}V1}$ (both immediately and after 30 min), while the increase in *Outdegree* for forward connections was significantly greater for the reverse ccPAS$_{V1\text{-}STS}$ protocol only after 30 min.

Statistical results for all comparisons of Fig. 4 are summarized in Table 1 (including *t*-statistics, *p*-values, Cohen's *d*, and partial eta-squared η_p^2). For all statistically significant comparisons (corrected $p<0.05$; highlighted in bold in the table), effect size estimates revealed large magnitudes ($|\text{Cohen's } d|>0.79$, up to 1.31; $\eta_p^2>0.40$, up to 0.64). These findings suggest that the observed modulations are robust and likely reflect underlying changes in connectivity.

The same analyses were repeated for the single frequency bands: theta, alpha, beta, and low-mid gamma. Results are depicted in Fig. 5, Fig. 6, Fig. 7 and Fig. 8. In general, the different frequency bands replicate the overall behavior of the entire 4–80 Hz band. Nonetheless, some interesting differences are noticeable. In particular, an increase in backward connections is also present for ccPAS$_{V1\text{-}STS}$ at *post$_{0min}$* in the theta band (Fig. 5, *panel b)*), while an increase in forward connections can also be seen in the gamma band immediately after ccPAS$_{STS\text{-}V1}$ (Fig. 8, *panel a)*). Regarding the theta band, however, after 30 min, the increase in backward connectivity following ccPAS$_{V1\text{-}STS}$ is smaller than the increase after ccPAS$_{STS\text{-}V1}$.

Statistical results for all comparisons across different frequency bands are reported in Table S1 of the *"Supplementary material"*.

The results of the within-clusters changes in *Outdegree* between the two sessions for the entire frequency-band are reported in the *"Supplementary material"*, Fig. S1. Notably, a significantly greater increase in connectivity is always observed in the "first" stimulated cluster. That is, the ccPAS$_{STS\text{-}V1}$ session mainly increases the connections internal to the temporoparietal cluster, whereas ccPAS$_{V1\text{-}STS}$ especially increases those internal to the occipital one.

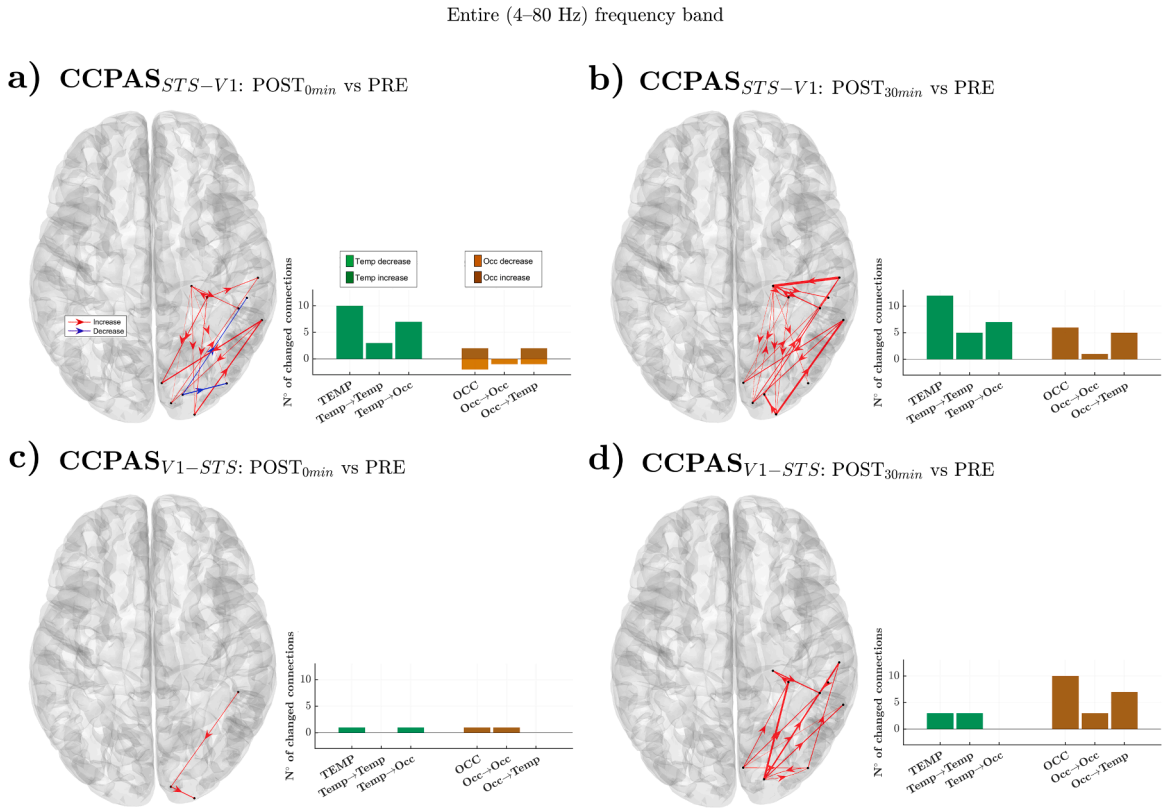

Fig. 3. *Functional connectivity changes across the entire frequency band.* Results are shown for all connections that exhibit significant (FDR BH-corrected) differences between *pre* and *post$_{0min}$* (left column) and *pre* and *post$_{30min}$* (right column), for both stimulation sessions. The top row corresponds to the ccPAS$_{STS\text{-}V1}$ protocol, the bottom row to the ccPAS$_{V1\text{-}STS}$ protocol. Red arrows indicate connections stronger after stimulation (*post$_{0min}$* or *post$_{30min}$*), blue arrows those stronger at *pre*, with arrow width proportional to the difference in connectivity values. Histograms next to the cortical maps display the number of significant connections: increases are plotted on the positive y-axis and decreases on the negative y-axis for each cluster. Connections are organized by directionality: in each histogram, we display the total number of connections (for the TEMP or OCC cluster), those internal to a cluster (Temp→Temp and Occ→Occ), and those connecting one cluster to the other (Temp→Occ and Occ→Temp). *ROIs* labels are omitted for clarity but are reported in Fig. 2. Since only the top view of the cortex is shown, the position of the ROIs has been slightly shifted from their original positions to make the graph clearer.

4. Discussion

We asked whether long-latency ccPAS over pSTS and V1/V2 can shape directional functional interactions within a lateral occipito-temporal circuit implicated in social and emotion perception (Borgomaneri et al., 2023; Pitcher and Ungerleider, 2021). To address this question, we repeatedly paired pSTS and V1/V2 stimulation, building on the long-latency communication delay between the two regions (from pSTS to V1/V2 (Borgomaneri et al., 2023)), and tested changes in connectivity using resting-state EEG combined with source-level, multivariate spectral Granger Causality analysis. Compared to more traditional metrics such as correlation or coherence, this approach allows estimation not only of the temporal and spectral aspects of cortical interactions but also of their directionality. It is therefore particularly suited to highlight the potential of ccPAS in modulating cortical dynamics in backward or forward directions.

Our results show that functional connectivity within the pSTS-V1/V2 circuit is malleable in a direction-specific manner. The ccPAS$_{\text{STS-V1}}$ protocol consistently enhanced backward (temporoparietal to occipital) connectivity, immediately after stimulation and 30 min later. We recognize that the immediate effects found at 0 min after ccPAS may reflect a combination of associative plasticity and non-specific factors (such as transient network perturbations) that do not indicate an already consolidated synaptic change. It is important to note, however, that the changes we observe at 0 min, particularly those involving backward connectivity, are fully confirmed at 30 min. This supports the interpretation that these effects already reflect the onset of plastic changes, whit later measurements at 30 min capturing their more consolidated expression. In contrast, changes in forward (occipital to temporoparietal) connectivity emerged only after 30 min, robustly after the reverse ccPAS$_{V1\text{-}STS}$ protocol and more weakly after ccPAS$_{STS\text{-}V1}$. Together, these results demonstrate that long-latency ccPAS can transiently bias the directionality of interactions in a putative "third" visual pathway linking pSTS with the visual cortex, in a time- and direction-dependent manner, with immediate effects confined to backward connectivity and delayed effects on forward connectivity, likely reflecting both specific and compensatory/homeostatic adjustments. Specifically, the *post$_{30min}$* resting-state recording occurred after additional experimental blocks (see the *"Methods"* section), which may have altered arousal, attention, or fatigue levels and thereby contributed to more global changes in connectivity. Importantly, however, the sequence and nature of these intervening blocks were identical in the ccPAS$_{STS\text{-}V1}$ and ccPAS$_{V1\text{-}STS}$ sessions, so any such global state fluctuations would be expected to affect both protocols and may therefore contribute to the non-specific component of the delayed forward increases observed across sessions.

Most prior ccPAS studies have used short interstimulus intervals (<10 ms) to strengthen direct cortico-cortical pathways, especially in the motor system (e.g., (Rizzo et al., 2009; Buch et al., 2011; Turrini et al., 2022, 2023a, 2023b, 2024; Bevacqua et al., 2024; Di Luzio et al., 2024; Breveglieri et al., 2025; Turrini et al., 2025) but see (Chiappini et al., 2020) for longer ISIs). Similarly, prior ccPAS applied over visual areas have commonly used ISIs tailored to short delay interactions between higher-order regions and early visual areas (Romei et al., 2016; Chiappini et al., 2018, 2022; Di Luzio et al., 2022; Bevilacqua et al.,

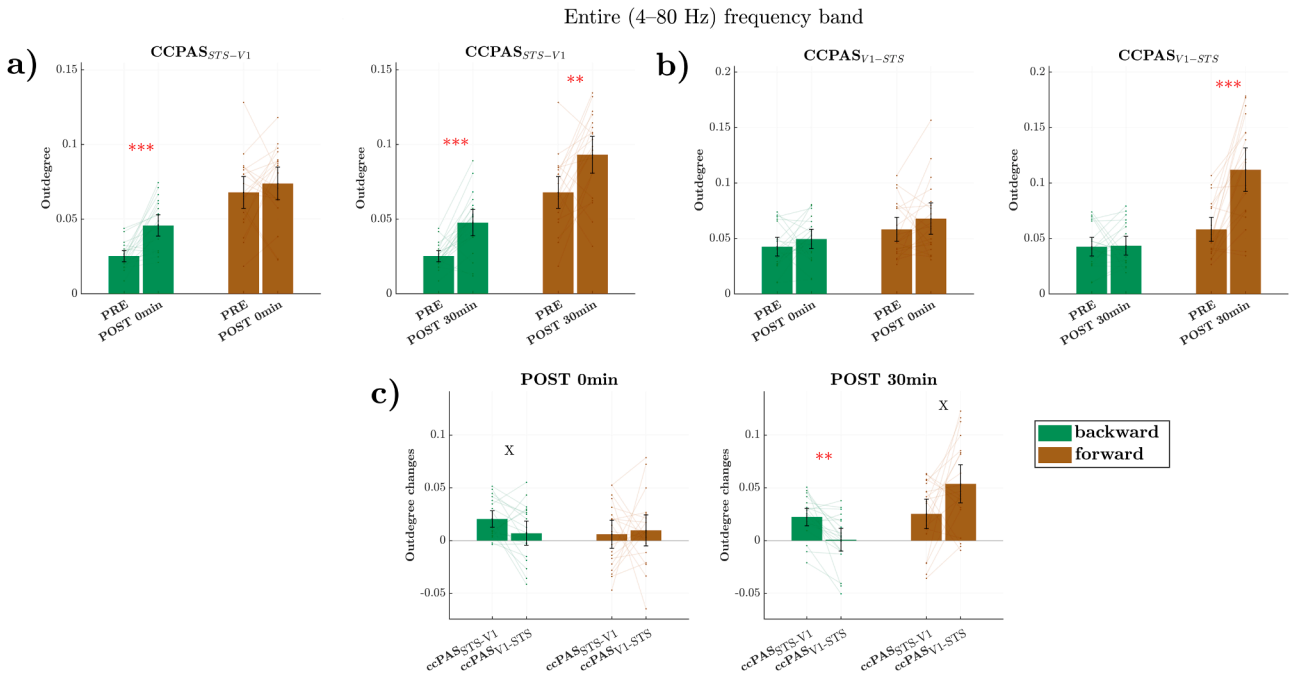

Fig. 4. *Statistical comparison of inter-cluster Outdegree values across time intervals and sessions for the entire frequency band. a) Outdegree* comparisons for ccPAS$_{STS\text{-}V1}$: *post$_{0min}$* vs *pre* (left column) and *post$_{30min}$* vs *pre* (right column). b) *Outdegree* comparisons for ccPAS$_{V1\text{-}STS}$. c) Comparison of *Outdegree* changes between the two protocols: ccPAS$_{STS\text{-}V1}$ vs ccPAS$_{V1\text{-}STS}$, at the two different time intervals: *post$_{0min}$* (left column) and *post$_{30min}$* (right column). Asterisks indicate significance (* $p < 0.05$, ** $p < 0.01$, *** $p < 0.001$; Bonferroni-corrected for 4 multiple comparisons). X denotes $p < 0.05$ (uncorrected). Error bars indicate 95% confidence intervals (CI). Faint lines represent individual participant trajectories.

Table 1
Statistical results of paired samples t-tests and effect size estimates for the entire frequency band (4–80 Hz). $t(19)$ indicates the *t*-statistic with 19 degrees of freedom. *p*-values are Bonferroni-corrected for 4 multiple comparisons. Cohen's *d* and partial eta-squared (η_p^2) provide effect size estimates. Statistically significant comparisons (corrected $p<0.05$) are highlighted in bold.

ENTIRE FREQUENCY RANGE (4–80 Hz)						
Session	Direction	Time interval	*t(19)*	*p-value (corrected)*	*Cohen's d*	η_p^2
ccPAS$_{STS\text{-}V1}$	**Backward**	**pre vs post0**	**−5.16**	**<0.001**	**−1.15**	**0.58**
	Forward	pre vs post0	−0.09	1.00	−0.20	0.04
	Backward	**pre vs post30**	**−5.29**	**<0.001**	**−1.18**	**0.60**
	Forward	**pre vs post30**	**−3.54**	**<0.01**	**−0.79**	**0.40**
ccPAS$_{V1\text{-}STS}$	Backward	pre vs post0	−1.19	1.00	−0.27	0.07
	Forward	pre vs post0	−1.30	0.84	−0.29	0.08
	Backward	pre vs post30	−0.16	1.00	−0.04	0.00
	Forward	**pre vs post30**	**−5.84**	**<0.001**	**−1.31**	**0.64**
ccPAS$_{STS\text{-}V1}$ vs ccPAS$_{V1\text{-}STS}$	Backward	pre vs post0	2.32	0.13	0.51	0.22
	Forward	pre vs post0	−0.34	1.00	−0.08	0.01
	Backward	**pre vs post30**	**3.96**	**<0.01**	**0.89**	**0.45**
	Forward	pre vs post30	−2.51	0.08	−0.56	0.25

2023, 2025) generally using ISIs below 20 ms. By contrast, our long-latency ccPAS with a 200-ms interval - derived from TMS–EEG estimates of pSTS-to-V1/V2 backward interactions (Borgomaneri et al., 2023) - was designed to engage indirect reentrant pathways, consistent with anatomical evidence that pSTS and early visual areas are mainly linked via polysynaptic routes (Driss Boussaoud et al., 1990; Kathleen S. Rockland and Van Hoesen, 1994; Weiner et al., 2016; Weiner and Gomez, 2021).

Previous application of this long-latency ccPAS$_{STS\text{-}V1}$ protocol showed improvements in emotion expression recognition, interpreted as reflecting strengthened backward connectivity (Borgomaneri et al., 2023; Cataneo et al., submitted). However, this interpretation was inferred indirectly from the order and timing of the paired pulses during ccPAS$_{STS\text{-}V1}$, as no direct connectivity metrics were assessed. Our resting-state EEG findings now fill this gap by providing direct evidence that long-latency ccPAS$_{STS_V1}$ uniquely induces an increase in backward functional connectivity at rest, an effect not observed with the reverse protocol. This indicates that Hebbian-like mechanisms can be recruited not only in monosynaptic circuits but also in long-range, polysynaptic reentrant pathways, and establishes that backward temporo-occipital projections are plastic and susceptible to timing-based neuromodulation when stimulation is aligned with their intrinsic communication delays.

By demonstrating that long-latency ccPAS directly enhances backward connectivity, our study provides the missing physiological link that complements prior behavioral and electrophysiological findings (Borgomaneri et al., 2023; Cataneo et al., submitted). Taken together, the evidence now clearly indicates that the backward pathway from pSTS to the visual cortex is not only malleable and sensitive to long-latency ccPAS, but also causally essential for the perception of emotional expressions. This supports a critical role of the lateral temporo-occipital "third" visual pathway in social perception (Pitcher and Ungerleider, 2021; Weiner and Gomez, 2021) and aligns with models emphasizing backward projections and iterative processing loops that challenge strictly feedforward views of visual architecture (Lamme and Roelfsema, 2000; Summerfield and de Lange, 2014; Michel et al., 2019). Notably, prior work showed that perceptual improvements

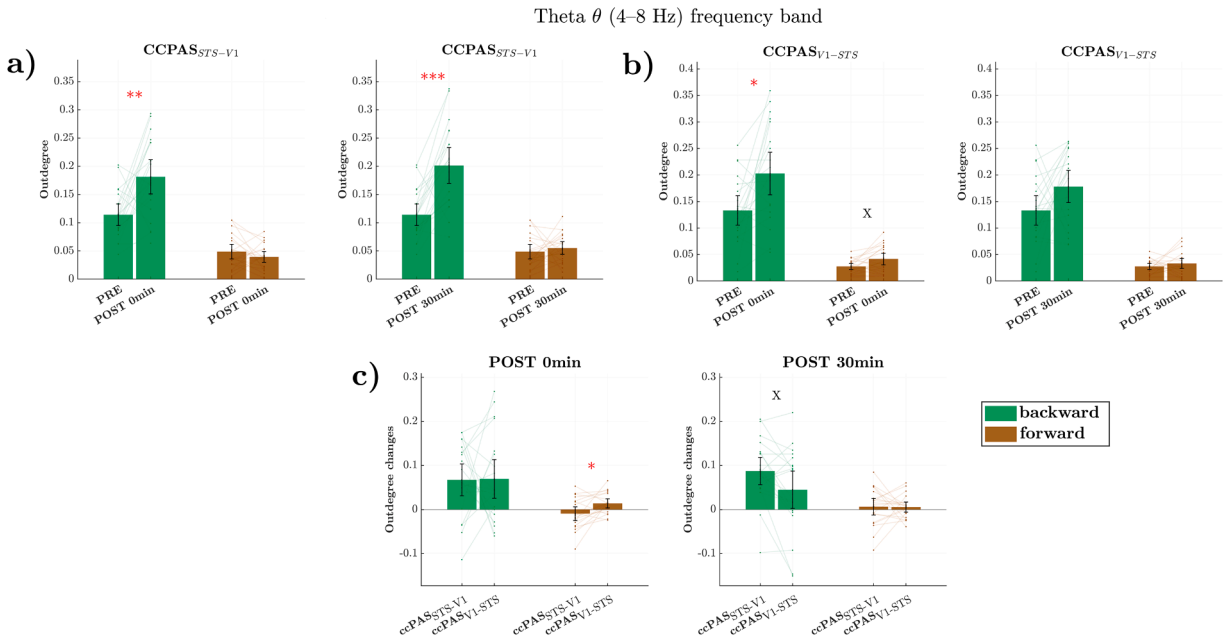

Fig. 5. *Statistical comparison of inter-cluster Outdegree values across time intervals and sessions for the theta band. a) Outdegree* comparisons for ccPAS$_{STS\text{-}V1}$: *post*$_{0min}$ vs *pre* (left column) and *post*$_{30min}$ vs *pre* (right column). *b) Outdegree* comparisons for ccPAS$_{V1\text{-}STS}$. *c)* Comparison of *Outdegree* changes between the two different protocols: ccPAS$_{STS\text{-}V1}$ vs ccPAS$_{V1\text{-}STS}$, at the two different time intervals: *post*$_{0min}$ (left column) and *post*$_{30min}$ (right column). Asterisks indicate significance (* $p < 0.05$, ** $p < 0.01$, *** $p < 0.001$; Bonferroni correction for 4 multiple comparisons). X denotes $p < 0.05$ (uncorrected). Error bars indicate 95% CI. Faint lines represent individual participant trajectories.

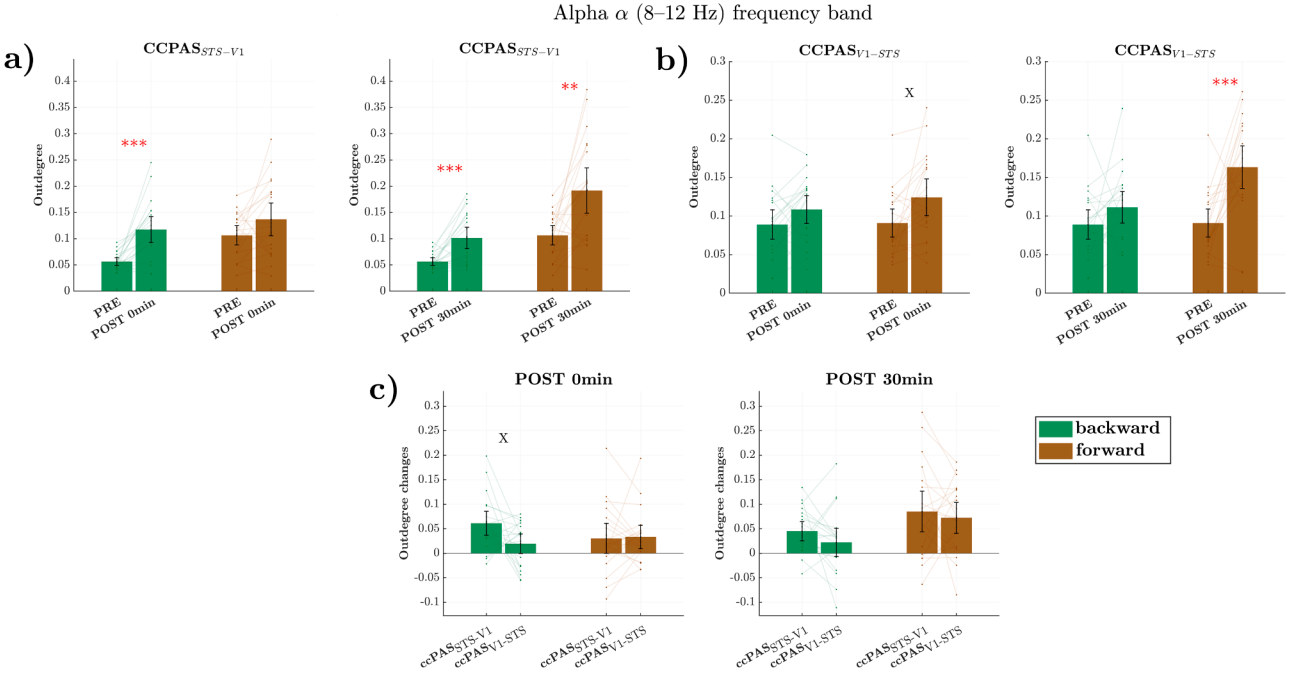

Fig. 6. *Statistical comparison of inter-cluster Outdegree values across time intervals and sessions for the alpha band. a) Outdegree* comparisons for ccPAS$_{STS\text{-}V1}$: *post*$_{0min}$ vs *pre* (left column) and *post*$_{30min}$ vs *pre* (right column). *b) Outdegree* comparisons for ccPAS$_{V1\text{-}STS}$. *c)* Comparison of *Outdegree* changes between the two different protocols: ccPAS$_{STS\text{-}V1}$ vs ccPAS$_{V1\text{-}STS}$, at the two different time intervals: *post*$_{0min}$ (left column) and *post*$_{30min}$ (right column). Asterisks indicate significance (* $p < 0.05$, ** $p < 0.01$, *** $p < 0.001$; Bonferroni correction for 4 multiple comparisons). X denotes $p < 0.05$ (uncorrected). Error bars indicate 95% CI. Faint lines represent individual participant trajectories.

following ccPAS$_{STS\text{-}V1}$ were restricted to emotional expression recognition and did not extend to gender judgments of the same faces (Borgomaneri et al., 2023; Cataneo et al., submitted), which rely on ventral occipito-temporal regions such as the fusiform gyrus (Haxby et al., 2000; Pitcher et al., 2011). This dissociation suggests that pSTS-to-V1/V2 feedback preferentially contributes to emotional aspects of face perception, whereas other facial attributes are likely mediated by distinct, parallel pathways.

Our study also highlights a striking asymmetry between the two stimulation protocols, likely due to the stimulation timing being

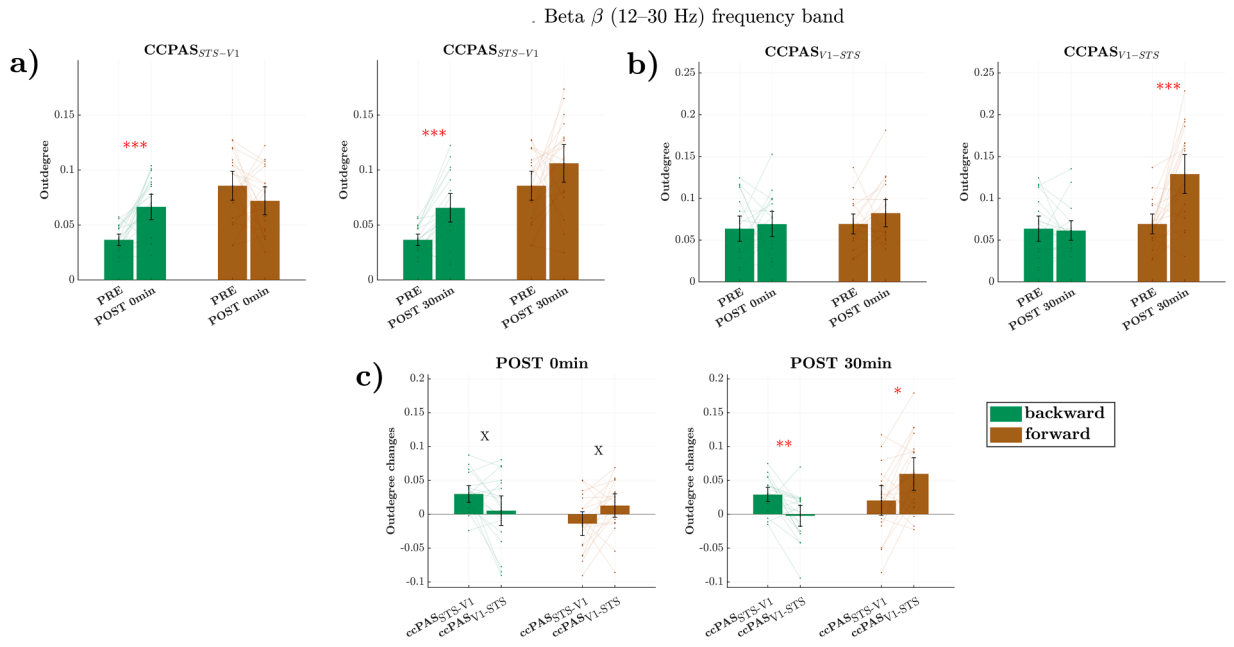

Fig. 7. *Statistical comparison of inter-cluster Outdegree values across time intervals and sessions for the beta band. a) Outdegree* comparisons for ccPAS$_{STS\text{-}V1}$: *post*$_{0min}$ vs *pre* (left column) and *post*$_{30min}$ vs *pre* (right column). *b) Outdegree* comparisons for ccPAS$_{V1\text{-}STS}$. *c)* Comparison of *Outdegree* changes between the two different protocols: ccPAS$_{STS\text{-}V1}$ vs ccPAS$_{V1\text{-}STS}$, at the two different time intervals: *post*$_{0min}$ (left column) and *post*$_{30min}$ (right column). Asterisks indicate significance (* $p < 0.05$, ** $p < 0.01$, *** $p < 0.001$; Bonferroni correction for 4 multiple comparisons). X denotes $p < 0.05$ (uncorrected). Error bars indicate 95% CI. Faint lines represent individual participant trajectories.

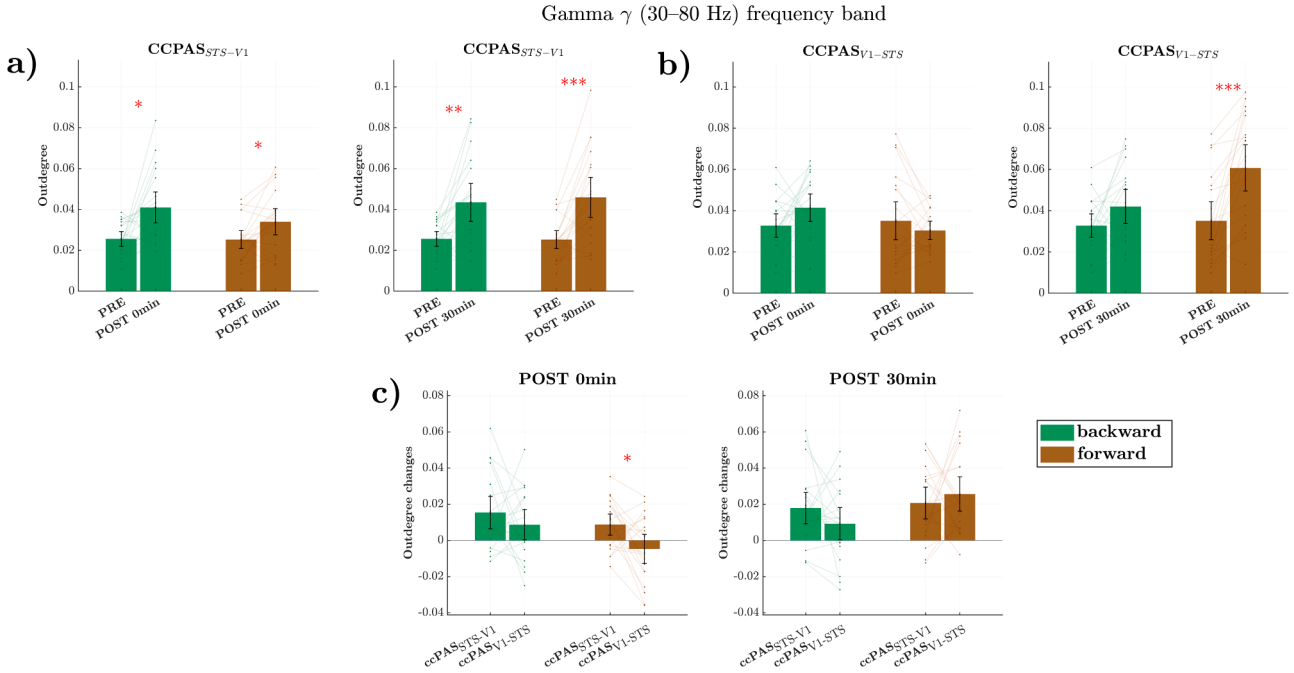

Fig. 8. *Statistical comparison of inter-cluster Outdegree values across time intervals and sessions for the gamma band. a) Outdegree* comparisons for ccPAS$_{STS\text{-}V1}$: *post*$_{0min}$ vs *pre* (left column) and *post*$_{30min}$ vs *pre* (right column). *b) Outdegree* comparisons for ccPAS$_{V1\text{-}STS}$. *c)* Comparison of *Outdegree* changes between the two different protocols: ccPAS$_{STS\text{-}V1}$ vs ccPAS$_{V1\text{-}STS}$, at the two different time intervals: *post*$_{0min}$ (left column) and *post*$_{30min}$ (right column). Asterisks indicate significance (* $p < 0.05$, ** $p < 0.01$, *** $p < 0.001$; Bonferroni correction for 4 multiple comparisons). X denotes $p < 0.05$ (uncorrected). Error bars indicate 95% CI. Faint lines represent individual participant trajectories.

optimized for the physiological delay of the backward pSTS-to-V1/V2 pathway rather than the forward V1/V2-to-pSTS pathway (Borgomaneri et al., 2023). While ccPAS$_{STS\text{-}V1}$ rapidly enhanced backward connectivity, with effects persisting at *post*$_{30min}$, changes in forward interactions were delayed and likely reflected a combination of protocol-specific and non-specific effects. Increases in forward connectivity emerged only 30 min after stimulation and were stronger following ccPAS$_{V1\text{-}STS}$, with weaker effects also present after ccPAS$_{STS\text{-}V1}$. This delayed pattern is compatible with secondary, network-level adjustments and possibly homeostatic mechanisms, but

alternative explanations, including unspecific TMS effects and broader fluctuations in brain state, cannot be ruled out with the present design. Similar compensatory mechanisms have been proposed in other studies using both short- and longer-latency ccPAS protocols (e.g., (Johnen et al., 2015; Chiappini et al., 2020)). This pattern of findings underscores a temporal asymmetry in long-latency ccPAS effects, with immediate Hebbian-like potentiation confined to the targeted backward pathway, and delayed forward changes arising from a mixture of protocol-specific and secondary network-level adjustments.

Frequency-band analyses were broadly consistent with these directional effects across multiple oscillatory bands, but also revealed nuances. The presence of enhanced backward connectivity in the theta band following $ccPAS_{V1\_STS}$ and the enhancement of forward connections in the gamma band following $ccPAS_{STS\_V1}$ - both observed immediately post-stimulation - suggest that both lower- and higher-frequency oscillations may exhibit a different sensitivity to ccPAS interventions. Importantly, these frequency-specific effects merit further investigation, as they may reflect the involvement of different oscillatory mechanisms. For example, slower theta oscillations have been often associated with long-range coordination and top-down control of sensory processing, while the faster gamma activity is commonly believed to be involved in bottom-up, feedforward transmission of information along visual pathways (Fries, 2005; Cavanagh and Frank, 2014; Bastos et al., 2015; Michalareas et al., 2016).

The present methodology offers promising applications for future investigations of associative plasticity within different brain networks and may guide the development of specific neuromodulatory interventions aimed at restoring optimal cortical function in clinical populations. For example, the ability to selectively strengthen specific functional pathways may prove valuable in addressing emotion perception deficits observed in various neuropsychiatric or neuropsychological disorders (e.g. (Kohler et al., 2004; Bediou et al., 2012; Narme et al., 2013)).

Some limitations should be acknowledged. Our post-stimulation evaluation window was limited to 30 min, preventing conclusions about the long-term persistence of these connectivity changes. Yet, based on behavioral (Borgomaneri et al., 2023) and electrophysiological findings (Cataneo et al., submitted) we may expect changes to persist for at least 80 min post-stimulation. We administered the same 200-ms ISI - estimated to manipulate backward pSTS-to-V1/V2 connectivity (Borgomaneri et al., 2023) - in the reverse $ccPAS_{V1\_STS}$ protocol. Yet, feedforward communication is thought to occur more rapidly than feedback (Semedo et al., 2022). Therefore, future studies should determine the specific effect duration of long-latency ccPAS on connectivity, whether $ccPAS_{V1\_STS}$ delivered with shorter ISIs tailored to forward interactions can more effectively modulate connectivity along the V1/V2-to-pSTS direction. The present work was specifically designed to characterize ccPAS-induced changes in resting-state connectivity, future studies should integrate these measures with behavioral indices of social perception at the single-subject level, to clarify how individual differences in ccPAS-induced connectivity changes relate to behavioral changes. The absence of a sham ccPAS session and the presence of intervening tasks between the immediate and 30 min recordings prevent us from determining whether delayed forward changes reflect compensatory plasticity, non-specific TMS effects, or global state fluctuations. Future studies could also benefit from electric-filed modelling or individualized intensity calibration to further refine pathway-specific ccPAS protocols. Finally, although participants denied any history of psychiatric conditions or psychotropic medication use, we did not administer standardized questionnaires for subclinical mood or anxiety (e.g., BDI, STAI). Since individual differences in anxiety or depression can modulate neural responses to emotional faces in occipito-temporal regions, including areas within the pSTS-visual network (e.g. (Gentili et al., 2015; Kustubayeva et al., 2023)), future work should include such measures to better characterize their potential influence on connectivity.

In summary, our study demonstrates that long-latency ccPAS can causally and selectively modulate the directionality of connectivity between pSTS and the visual cortex. By applying a 200-ms ISI tuned to the intrinsic delay of the reentrant pathway (Borgomaneri et al., 2023), we observed robust and persistent enhancement of temporo-occipital backward connectivity, accompanied by delayed and weaker adjustments in the opposite forward direction. These results extend previous behavioral findings by providing direct physiological evidence that temporo-occipital backward projections are plastic and susceptible to timing-based neuromodulation. More broadly, together with prior behavioral findings (Borgomaneri et al., 2023; Cataneo et al., submitted) these findings suggest a key role of feedback signals within the lateral "third" visual pathway, challenging strictly feedforward accounts of visual perception. The asymmetry between backward and forward effects further underscores the importance of pathway-specific delays in shaping ccPAS outcomes, and calls for future work to refine stimulation parameters for optimal targeting of distinct cortico-cortical routes. Together, these findings establish long-latency ccPAS as a powerful tool to probe and modulate large-scale reentrant circuits, advancing our understanding of the neural mechanisms that support social and emotional vision.

CRediT authorship contribution statement

Gabriele Pirazzini: Writing – review & editing, Writing – original draft, Visualization, Software, Methodology, Formal analysis, Data curation. **Antonio Cataneo:** Writing – review & editing, Visualization, Validation, Methodology, Investigation, Data curation. **Silvana Pelle:** Writing – review & editing, Visualization, Software, Methodology, Formal analysis, Data curation. **Alice Marra:** Writing – review & editing, Validation, Methodology, Investigation, Data curation. **Giorgio Arcara:** Writing – review & editing, Supervision, Software, Methodology, Conceptualization. **Simone Battaglia:** Writing – review & editing, Validation, Project administration, Methodology, Investigation, Funding acquisition, Data curation, Conceptualization. **Mauro Ursino:** Writing – review & editing, Writing – original draft, Validation, Supervision, Software, Resources, Project administration, Methodology, Funding acquisition. **Alessio Avenanti:** Writing – review & editing, Writing – original draft, Validation, Supervision, Resources, Project administration, Methodology, Funding acquisition, Conceptualization.

Declaration of competing interest

The authors declare that they have no known competing interests.

Acknowledgments

Research supported by #NEXTGENERATIONEU (NGEU) and funded by the Ministry of University and Research (MUR), National Recovery and Resilience Plan (NRRP), project MNESYS (PE0000006)—A Multiscale integrated approach to the study of the nervous system in health and disease (DN. 1553 11.10.2022); and Bial Foundation, Portugal (235/22).

Supplementary materials

Supplementary material associated with this article can be found, in the online version, at doi:10.1016/j.neuroimage.2026.121759.

References

Avenanti, A., Annela, L., Serino, A., 2012. Suppression of premotor cortex disrupts motor coding of peripersonal space. Neuroimage 63, 281–288. https://doi.org/10.1016/j.neuroimage.2012.06.063.

Avenanti, A., Annella, L., Candidi, M., Urgesi, C., Aglioti, S.M., 2013. Compensatory plasticity in the action observation network: virtual lesions of STS enhance

anticipatory simulation of seen actions. Cereb. Cortex. 23, 570–580. https://doi.org/10.1093/cercor/bhs040.
Barnett, L., Seth, A.K., 2014. The MVGC multivariate Granger causality toolbox: a new approach to Granger-causal inference. J. Neurosci. Methods 223, 50–68. https://doi.org/10.1016/j.jneumeth.2013.10.018.
Bastos, A.M., Vezoli, J., Bosman, C.A., Schoffelen, J.-M., Oostenveld, R., Dowdall, J.R., De Weerd, P., Kennedy, H., Fries, P., 2015. Visual areas exert feedforward and feedback influences through distinct frequency channels. Neuron 85, 390–401. https://doi.org/10.1016/j.neuron.2014.12.018.
Bediou, B., Brunelin, J., d'Amato, T., Fecteau, S., Saoud, M., Hénaff, M.-A., Krolak-Salmon, P., 2012. A comparison of facial emotion processing in neurological and psychiatric conditions. Front. Psychol. 3. https://doi.org/10.3389/fpsyg.2012.00098.
Bell, A.J., Sejnowski, T.J., 1995. An information-maximization approach to blind separation and blind deconvolution. Neural Comput. 7, 1129–1159. https://doi.org/10.1162/neco.1995.7.6.1129.
Benjamini, Y., Hochberg, Y., 1995. Controlling the false discovery rate: a practical and powerful approach to multiple testing. J. R. Stat. Soc. B. 57, 289–300.
Bertini, C., Leo, F., Avenanti, A., Làdavas, E., 2010. Independent mechanisms for ventriloquism and multisensory integration as revealed by theta-burst stimulation. Eur. J. Neurosci. 31, 1791–1799. https://doi.org/10.1111/j.1460-9568.2010.07200.x.
Bevacqua, N., Turrini, S., Fiori, F., Saracini, C., Lucero, B., Candidi, M., Avenanti, A., 2024. Cortico-cortical paired associative stimulation highlights asymmetrical communication between rostral premotor cortices and primary motor cortex. Brain Stimul. Basic Transl. Clin. Res. Neuromodulation. 17, 89–91. https://doi.org/10.1016/j.brs.2024.01.001.
Bevilacqua, M., Huxlin, K.R., Hummel, F.C., Raffin, E., 2023. Pathway and directional specificity of Hebbian plasticity in the cortical visual motion processing network. iScience 26. https://doi.org/10.1016/j.isci.2023.107064.
Bevilacqua, M., Windel, F., Beanato, E., Menoud, P., Zandvliet, S., Ramdass, N., Fleury, L., Hervé, J., Huxlin, K.R., Hummel, F.C., Raffin, E., 2025. Pathway-dependent brain stimulation responses indicate motion processing integrity after stroke. Brain 148, 2361–2372. https://doi.org/10.1093/brain/awaf043.
Borgomaneri, S., Zanon, M., Di Luzio, P., Cataneo, A., Arcara, G., Romei, V., Tamietto, M., Avenanti, A., 2023. Increasing associative plasticity in temporo-occipital back-projections improves visual perception of emotions. Nat. Commun. 14, 5720. https://doi.org/10.1038/s41467-023-41058-3.
Boussaoud, D., Ungerleider, L.G., Desimone, R., 1990a. Pathways for motion analysis: cortical connections of the medial superior temporal and fundus of the superior temporal visual areas in the macaque. J. Comp. Neurol. 296, 462–495. https://doi.org/10.1002/cne.902960311.
Boussaoud, D., Ungerleider, L.G., Desimone, R., 1990b. Pathways for motion analysis: cortical connections of the medial superior temporal and fundus of the superior temporal visual areas in the macaque. J. Comp. Neurol. 296, 462–495. https://doi.org/10.1002/cne.902960311.
Breveglieri, R., Bosco, A., Borgomaneri, S., Tessari, A., Galletti, C., Avenanti, A., Fattori, P., 2021. Transcranial magnetic stimulation over the Human medial posterior parietal cortex disrupts depth encoding during reach planning. Cereb. Cortex. 31, 267–280. https://doi.org/10.1093/cercor/bhaa224.
Breveglieri, R., Brandolani, R., Galletti, C., Avenanti, A., Fattori, P., 2025. Time-dependent enhancement of corticospinal excitability during cortico-cortical paired associative stimulation of the hV6A-M1 network in the human brain. Neuroimage 316, 121301. https://doi.org/10.1016/j.neuroimage.2025.121301.
Buch, E.R., Johnen, V.M., Nelissen, N., O'Shea, J., Rushworth, M.F.S., 2011. Noninvasive associative plasticity induction in a corticocortical pathway of the Human brain. J. Neurosci. 31, 17669–17679. https://doi.org/10.1523/JNEUROSCI.1513-11.2011.
Candidi, M., Stienen, B.M.C., Aglioti, S.M., de Gelder, B., 2015. Virtual lesion of right posterior superior temporal sulcus modulates conscious visual perception of fearful expressions in faces and bodies. Cortex 65, 184–194. https://doi.org/10.1016/j.cortex.2015.01.012.
Caporale, N., Dan, Y., 2008. Spike timing–Dependent plasticity: a Hebbian learning rule. Annu Rev. Neurosci. 31, 25–46. https://doi.org/10.1146/annurev.neuro.31.060407.125639.
Cataneo A., Battaglia S., Zanon M., Marra A., Lago S., Arcara G., Romei V., Tamietto M., Borgomaneri S., & Avenanti A. (submitted). Electrophysiological evidence for task-dependent and sustained associative plasticity through Hebbian strengthening of temporo-occipital backprojections.
Cavanagh, J.F., Frank, M.J., 2014. Frontal theta as a mechanism for cognitive control. Trends. Cogn. Sci. 18, 414–421. https://doi.org/10.1016/j.tics.2014.04.012.
Chiappini, E., Borgomaneri, S., Marangon, M., Turrini, S., Romei, V., Avenanti, A., 2020. Driving associative plasticity in premotor-motor connections through a novel paired associative stimulation based on long-latency cortico-cortical interactions. Brain. Stimul. Basic Transl. Clin. Res. Neuromodulation. 13, 1461–1463. https://doi.org/10.1016/j.brs.2020.08.003.
Chiappini, E., Sel, A., Hibbard, P.B., Avenanti, A., Romei, V., 2022. Increasing interhemispheric connectivity between human visual motion areas uncovers asymmetric sensitivity to horizontal motion. Curr. Biol. 32, 4064–4070. https://doi.org/10.1016/j.cub.2022.07.050 e3.
Chiappini, E., Silvanto, J., Hibbard, P.B., Avenanti, A., Romei, V., 2018. Strengthening functionally specific neural pathways with transcranial brain stimulation. Curr. Biol. 28, R735–R736. https://doi.org/10.1016/j.cub.2018.05.083.
Delorme, A., Makeig, S., 2004. EEGLAB: an open source toolbox for analysis of single-trial EEG dynamics including independent component analysis. J. Neurosci. Methods 134, 9–21. https://doi.org/10.1016/j.jneumeth.2003.10.009.
Di Luzio, P., Brady, L., Turrini, S., Romei, V., Avenanti, A., Sel, A., 2024. Investigating the effects of cortico-cortical paired associative stimulation in the human brain: a systematic review and meta-analysis. Neurosci. Biobehav. Rev. 167, 105933. https://doi.org/10.1016/j.neubiorev.2024.105933.
Distler, C., Boussaoud, D., Desimone, R., Ungerleider, L.G., 1993. Cortical connections of inferior temporal area TEO in macaque monkeys. J. Comp. Neurol. 334, 125–150. https://doi.org/10.1002/cne.903340111.
Dricu, M., Frühholz, S., 2016. Perceiving emotional expressions in others: activation likelihood estimation meta-analyses of explicit evaluation, passive perception and incidental perception of emotions. Neurosci. Biobehav. Rev. 71, 810–828. https://doi.org/10.1016/j.neubiorev.2016.10.020.
Fan, L., Li, H., Zhuo, J., Zhang, Y., Wang, J., Chen, L., Yang, Z., Chu, C., Xie, S., Laird, A. R., Fox, P.T., Eickhoff, S.B., Yu, C., Jiang, T., 2016. The Human brainnetome Atlas: a new brain atlas based on connectional architecture. Cereb. Cortex. 26, 3508–3526. https://doi.org/10.1093/cercor/bhw157.
Farahani, F.V., Karwowski, W., Lighthall, N.R., 2019. Application of graph theory for identifying connectivity patterns in Human brain networks: a systematic review. Front. Neurosci. 13, 585. https://doi.org/10.3389/fnins.2019.00585.
Ferrari, C., Schiavi, S., Cattaneo, Z., 2018. TMS over the superior temporal sulcus affects expressivity evaluation of portraits. Cogn. Affect. Behav. Neurosci. 18, 1188–1197. https://doi.org/10.3758/s13415-018-0630-4.
Fiori, F., Chiappini, E., Avenanti, A., 2018. Enhanced action performance following TMS manipulation of associative plasticity in ventral premotor-motor pathway. Neuroimage 183, 847–858. https://doi.org/10.1016/j.neuroimage.2018.09.002.
Fries, P., 2005. A mechanism for cognitive dynamics: neuronal communication through neuronal coherence. Trends. Cogn. Sci. 9, 474–480. https://doi.org/10.1016/j.tics.2005.08.011.
Gentili, C., Vanello, N., Cristea, I., David, D., Ricciardi, E., Pietrini, P., 2015. Proneness to social anxiety modulates neural complexity in the absence of exposure: a resting state fMRI study using Hurst exponent. Psychiatry Res. NeuroimAging 232, 135–144. https://doi.org/10.1016/j.pscychresns.2015.03.005.
Ginter, J., Blinowska, K.J., Kamiński, M., Durka, P.J., 2001. Phase and amplitude analysis in time–frequency space—application to voluntary finger movement. J. Neurosci. Methods 110, 113–124. https://doi.org/10.1016/S0165-0270(01)00424-1.
Gramfort, A., Papadopoulo, T., Olivi, E., Clerc, M., 2010. OpenMEEG: opensource software for quasistatic bioelectromagnetics. Biomed. Eng. Online 9, 45. https://doi.org/10.1186/1475-925X-9-45.
Haxby, J.V., Hoffman, E.A., Gobbini, M.I., Haxby, J.V., Hoffman, E.A., Gobbini, M.I., Haxby, J.V., Hoffman, E.A., Gobbini, M.I., 2000. The distributed human neural system for face perception. Trends. Cogn. Sci. 4, 223–233. https://doi.org/10.1016/S1364-6613(00)01482-0.
Hernandez-Pavon, J.C., San Agustín, A., Wang, M.C., Veniero, D., Pons, J.L., 2023a. Can we manipulate brain connectivity? a systematic review of cortico-cortical paired associative stimulation effects. Clin. Neurophysiol. 154, 169–193. https://doi.org/10.1016/j.clinph.2023.06.016.
Hernandez-Pavon, J.C., Schneider-Garces, N., Begnoche, J.P., Miller, L.E., Raij, T., 2023b. Targeted modulation of human brain interregional effective connectivity with spike-timing dependent plasticity. Neuromodulation. Technol. Neural Interface 26, 745–754. https://doi.org/10.1016/j.neurom.2022.10.045.
Hlaváčková-Schindler, K., Plant, C., 2020. Heterogeneous graphical granger causality by minimum message length. Entropy 22, 1400. https://doi.org/10.3390/e22121400.
Huang, D., Ren, A., Shang, J., Lei, Q., Zhang, Y., Yin, Z., Li, J., von Deneen, K.M., Huang, L., 2016. Combining partial directed coherence and graph theory to analyse effective brain networks of different mental tasks. Front. Hum. Neurosci. 10. https://doi.org/10.3389/fnhum.2016.00235.
Johnen, V.M., Neubert, F.-X., Buch, E.R., Verhagen, L., O'Reilly, J.X., Mars, R.B., Rushworth, M.F.S., 2015. Causal manipulation of functional connectivity in a specific neural pathway during behaviour and at rest. Elife 4, e04585. https://doi.org/10.7554/eLife.04585.
Kohler, C.G., Turner, T.H., Gur, R.E., Gur, R.C., 2004. Recognition of facial emotions in neuropsychiatric disorders. CNS. Spectr. 9, 267–274. https://doi.org/10.1017/S1092852900009202.
Kustubayeva, A., Eliassen, J., Matthews, G., 2023. FMRI study of implicit emotional face processing in patients with MDD with melancholic subtype. Front. Hum. Neurosci. 17. https://doi.org/10.3389/fnhum.2023.1029789.
Lamme, V.A.F., Roelfsema, P.R., 2000. The distinct modes of vision offered by feedforward and recurrent processing. Trends. Neurosci. 23, 571–579. https://doi.org/10.1016/S0166-2236(00)01657-X.
Luzio, P.D., Tarasi, L., Silvanto, J., Avenanti, A., Romei, V., 2022. Human perceptual and metacognitive decision-making rely on distinct brain networks. PLoS. Biol. 20, e3001750. https://doi.org/10.1371/journal.pbio.3001750.
Metropolis, N., Ulam, S., 1949. The Monte Carlo method. J. Am. Stat. Assoc. 44, 335–341. https://doi.org/10.1080/01621459.1949.10483310.
Michalareas, G., Vezoli, J., van Pelt, S., Schoffelen, J.-M., Kennedy, H., Fries, P., 2016. Alpha-beta and gamma rhythms subserve feedback and feedforward influences among Human visual cortical areas. Neuron 89, 384–397. https://doi.org/10.1016/j.neuron.2015.12.018.
Michel, M., Beck, D., Block, N., Blumenfeld, H., Brown, R., Carmel, D., Carrasco, M., Chirimuuta, M., Chun, M., Cleeremans, A., Dehaene, S., Fleming, S.M., Frith, C., Haggard, P., He, B.J., Heyes, C., Goodale, M.A., Irvine, L., Kawato, M., Kentridge, R., King, J.-R., Knight, R.T., Kouider, S., Lamme, V., Lamy, D., Lau, H., Laureys, S., LeDoux, J., Lin, Y.-T., Liu, K., Macknik, S.L., Martinez-Conde, S., Mashour, G.A., Melloni, L., Miracchi, L., Mylopoulos, M., Naccache, L., Owen, A.M., Passingham, R. E., Pessoa, L., Peters, M.A.K., Rahnev, D., Ro, T., Rosenthal, D., Sasaki, Y., Sergent, C., Solovey, G., Schiff, N.D., Seth, A., Tallon-Baudry, C., Tamietto, M.,

Tong, F., van Gaal, S., Vlassova, A., Watanabe, T., Weisberg, J., Yan, K., Yoshida, M., 2019. Opportunities and challenges for a maturing science of consciousness. Nat. Hum. Behav. 3, 104–107. https://doi.org/10.1038/s41562-019-0531-8.

Milner, A.D., Goodale, M.A., 2006. The Visual Brain in Action, 2nd ed. Oxford University Press, New York, NY, US. https://doi.org/10.1093/acprof:oso/9780198524724.001.0001.

Minati, L., Varotto, G., D'Incerti, L., Panzica, F., Chan, D., 2013. From brain topography to brain topology: relevance of graph theory to functional neuroscience. Neuroreport 24, 536. https://doi.org/10.1097/WNR.0b013e3283621234.

Narme, P., Mouras, H., Roussel, M., Duru, C., Krystkowiak, P., Godefroy, O., 2013. Emotional and cognitive social processes are impaired in Parkinson's disease and are related to behavioral disorders. Neuropsychology 27, 182–192. https://doi.org/10.1037/a0031522.

Paracampo, R., Pirruccio, M., Costa, M., Borgomaneri, S., Avenanti, A., 2018. Visual, sensorimotor and cognitive routes to understanding others' enjoyment: an individual differences rTMS approach to empathic accuracy. Neuropsychol. Spec. Issue Neurosci. Empathy 116, 86–98. https://doi.org/10.1016/j.neuropsychologia.2018.01.043.

Pascual-Marqui, R.D., 2002. Standardized low-resolution brain electromagnetic tomography (sLORETA): technical details. Methods Find. Exp. Clin. Pharmacol. 24, 5–12. Suppl D.

Pelle, S., Piermaria, G., Magosso, E., Ursino, M., 2025. On the virtues and limitations of Granger-causal brain connectivity estimate: critical analysis using neural mass models. Netw. Neurosci. 1–24. https://doi.org/10.1162/netn.a.38.

Pirazzini, G., Starita, F., Ricci, G., Garofalo, S., di Pellegrino, G., Magosso, E., Ursino, M., 2023. Changes in brain rhythms and connectivity tracking fear acquisition and reversal. Brain Struct. Funct. 228, 1259–1281. https://doi.org/10.1007/s00429-023-02646-7.

Pitcher, D., 2014. Facial expression recognition takes longer in the posterior superior temporal sulcus than in the occipital face area. J. Neurosci. 34, 9173–9177. https://doi.org/10.1523/JNEUROSCI.5038-13.2014.

Pitcher, D., Ungerleider, L.G., 2021. Evidence for a third visual pathway specialized for social perception. Trends. Cogn. Sci. 25, 100–110. https://doi.org/10.1016/j.tics.2020.11.006.

Pitcher, D., Walsh, V., Duchaine, B., 2011. The role of the occipital face area in the cortical face perception network. Exp. Brain Res. 209, 481–493. https://doi.org/10.1007/s00221-011-2579-1.

Rizzo, V., Siebner, H.S., Morgante, F., Mastroeni, C., Girlanda, P., Quartarone, A., 2009. Paired associative stimulation of left and right Human motor cortex shapes interhemispheric motor inhibition based on a hebbian mechanism. Cereb. Cortex. 19, 907–915. https://doi.org/10.1093/cercor/bhn144.

Rockland, K.S., Van Hoesen, G.W., 1994a. Direct temporal-occipital feedback connections to striate cortex (V1) in the macaque monkey. Cereb. Cortex. 4, 300–313. https://doi.org/10.1093/cercor/4.3.300.

Rockland, K.S., Van Hoesen, G.W., 1994b. Direct temporal-occipital feedback connections to striate cortex (V1) in the Macaque monkey. Cereb. Cortex. 4, 300–313. https://doi.org/10.1093/cercor/4.3.300.

Romei, V., Chiappini, E., Hibbard, P.B., Avenanti, A., 2016. Empowering reentrant projections from V5 to V1 boosts sensitivity to motion. Curr. Biol. 26, 2155–2160. https://doi.org/10.1016/j.cub.2016.06.009.

Rossi, S., Antal, A., Bestmann, S., Bikson, M., Brewer, C., Brockmöller, J., Carpenter, L.L., Cincotta, M., Chen, R., Daskalakis, J.D., Di Lazzaro, V., Fox, M.D., George, M.S., Gilbert, D., Kimiskidis, V.K., Koch, G., Ilmoniemi, R.J., Lefaucheur, J.P., Leocani, L., Lisanby, S.H., Miniussi, C., Padberg, F., Pascual-Leone, A., Paulus, W., Peterchev, A. V., Quartarone, A., Rotenberg, A., Rothwell, J., Rossini, P.M., Santarnecchi, E., Shafi, M.M., Siebner, H.R., Ugawa, Y., Wassermann, E.M., Zangen, A., Ziemann, U., Hallett, M., 2021. Safety and recommendations for TMS use in healthy subjects and patient populations, with updates on training, ethical and regulatory issues: expert Guidelines. Clin. Neurophysiol. 132, 269–306. https://doi.org/10.1016/j.clinph.2020.10.003.

Rossi, S., Hallett, M., Rossini, P.M., Pascual-Leone, A., 2009. Safety, ethical considerations, and application guidelines for the use of transcranial magnetic stimulation in clinical practice and research. Clin. Neurophysiol. 120, 2008–2039. https://doi.org/10.1016/j.clinph.2009.08.016.

Rubinov, M., Sporns, O., 2010. Complex network measures of brain connectivity: uses and interpretations. Neuroimage Comput. Models Brain. 52, 1059–1069. https://doi.org/10.1016/j.neuroimage.2009.10.003.

Semedo, J.D., Jasper, A.I., Zandvakili, A., Krishna, A., Aschner, A., Machens, C.K., Kohn, A., Yu, B.M., 2022. Feedforward and feedback interactions between visual cortical areas use different population activity patterns. Nat. Commun. 13, 1099. https://doi.org/10.1038/s41467-022-28552-w.

Seth, A.K., Barrett, A.B., Barnett, L., 2015. Granger Causality analysis in neuroscience and neuroimaging. J. Neurosci. 35, 3293–3297. https://doi.org/10.1523/JNEUROSCI.4399-14.2015.

Summerfield, C., de Lange, F.P., 2014. Expectation in perceptual decision making: neural and computational mechanisms. Nat. Rev. Neurosci. 15, 745–756. https://doi.org/10.1038/nrn3838.

Tadel, F., Baillet, S., Mosher, J.C., Pantazis, D., Leahy, R.M., 2011. Brainstorm: a user-friendly application for MEG/EEG analysis. Comput. Intell. Neurosci. 2011, 879716. https://doi.org/10.1155/2011/879716.

Tarasi, L., Turrini, S., Sel, A., Avenanti, A., Romei, V., 2024. Cortico-cortical paired-associative stimulation to investigate the plasticity of cortico-cortical visual networks in humans. Curr. Opin. Behav. Sci. 56, 101359. https://doi.org/10.1016/j.cobeha.2024.101359.

Tawakuli, A., Havers, B., Gulisano, V., Kaiser, D., Engel, T., 2025. Survey:time-series data preprocessing: a survey and an empirical analysis. J. Eng. Res. 13, 674–711. https://doi.org/10.1016/j.jer.2024.02.018.

Turrini, S., Avenanti, A., 2023. Understanding the sources of cortico-cortical paired associative stimulation (ccPAS) variability: unraveling target-specific and state-dependent influences. Clin. Neurophysiol. 156, 290–292. https://doi.org/10.1016/j.clinph.2023.08.019.

Turrini, S., Bevacqua, N., Cataneo, A., Chiappini, E., Fiori, F., Candidi, M., Avenanti, A., 2023a. Transcranial cortico-cortical paired associative stimulation (ccPAS) over ventral premotor-motor pathways enhances action performance and corticomotor excitability in young adults more than in elderly adults. Front. Aging Neurosci. 15. https://doi.org/10.3389/fnagi.2023.1119508.

Turrini, S., Fiori, F., Arcara, G., Romei, V., di Pellegrino, G., Avenanti, A., 2025. State-dependent associative plasticity highlights function-specific premotor-motor pathways crucial for arbitrary visuomotor mapping. Sci. Adv. 11, eadu4098. https://doi.org/10.1126/sciadv.adu4098.

Turrini, S., Fiori, F., Bevacqua, N., Saracini, C., Lucero, B., Candidi, M., Avenanti, A., 2024. Spike-timing-dependent plasticity induction reveals dissociable supplementary– and premotor–motor pathways to automatic imitation. Proc. Natl. Acad. Sci. 121, e2404925121. https://doi.org/10.1073/pnas.2404925121.

Turrini, S., Fiori, F., Chiappini, E., Lucero, B., Santarnecchi, E., Avenanti, A., 2023b. Cortico-cortical paired associative stimulation (ccPAS) over premotor-motor areas affects local circuitries in the human motor cortex via hebbian plasticity. Neuroimage 271, 120027. https://doi.org/10.1016/j.neuroimage.2023.120027.

Turrini, S., Fiori, F., Chiappini, E., Santarnecchi, E., Romei, V., Avenanti, A., 2022. Gradual enhancement of corticomotor excitability during cortico-cortical paired associative stimulation. Sci. Rep. 12, 14670. https://doi.org/10.1038/s41598-022-18774-9.

Ursino, M., Serra, M., Tarasi, L., Ricci, G., Magosso, E., Romei, V., 2022. Bottom-up vs. top-down connectivity imbalance in individuals with high-autistic traits: an electroencephalographic study. Front. Syst. Neurosci. 16. https://doi.org/10.3389/fnsys.2022.932128.

van den Heuvel, M.P., de Lange, S.C., Zalesky, A., Seguin, C., Yeo, B.T.T., Schmidt, R., 2017. Proportional thresholding in resting-state fMRI functional connectivity networks and consequences for patient-control connectome studies: issues and recommendations. Neuroimage 152, 437–449. https://doi.org/10.1016/j.neuroimage.2017.02.005.

van Mierlo, P., Lie, O., Staljanssens, W., Coito, A., Vulliémoz, S., 2018. Influence of time-series normalization, number of nodes, connectivity and graph measure selection on seizure-onset zone localization from intracranial EEG. Brain Topogr. 31, 753–766. https://doi.org/10.1007/s10548-018-0646-7.

Van Steen, M., 2010. Graph theory and complex networks. An Introduction 144 (1).

Wang, X., Song, Y., Zhen, Z., Liu, J., 2016. Functional integration of the posterior superior temporal sulcus correlates with facial expression recognition. Hum. Brain Mapp. 37, 1930–1940. https://doi.org/10.1002/hbm.23145.

Weiner, K.S., Gomez, J., 2021. Third visual pathway, anatomy, and cognition across species. Trends. Cogn. Sci. 25, 548–549. https://doi.org/10.1016/j.tics.2021.04.002.

Weiner, K.S., Jonas, J., Gomez, J., Maillard, L., Brissart, H., Hossu, G., Jacques, C., Loftus, D., Colnat-Coulbois, S., Stigliani, A., Barnett, M.A., Grill-Spector, K., Rossion, B., 2016. The face-processing network is resilient to focal resection of Human visual cortex. J. Neurosci. 36, 8425–8440. https://doi.org/10.1523/JNEUROSCI.4509-15.2016.

World Medical Association, 2013. World medical association declaration of helsinki: ethical principles for medical research involving human subjects. JAMA 310, 2191–2194. https://doi.org/10.1001/jama.2013.281053.